[1.]Ashwini MAHAKALKAR, [2.]Vinod VARGHESE

THERMOELASTIC BENDING ANALYSIS OF A SIMPLY-SUPPORTED RECTANGULAR PLATE EXPOSED TO POINT-IMPULSIVE SECTIONAL HEAT SUPPLY AMIDST A RECTANGULAR FRAME

[1.]Department of Mathematics, Mahatma Gandhi Science College, Armori, Gadchiroli, INDIA
[2.]Department of Mathematics, Smt. Sushilabai Bharti Science College, Arni, Yavatmal, INDIA

Abstract: An analysis of the unsteady-state three-dimensional heat conduction analysis of a rectangular plate is carried out by using a classical method. The boundary conditions for a temperature field are considered to be a partially prescribed temperature on the top face, zero temperature at the bottom face and four edges, and no flux at any edges. The intensities of bending moments, resultant moments and resultant forces are formulated based on the small-deflection theory and the analytical solution for the thermal stress components is obtained based on it. Numerical results for thermal stresses are presented. Furthermore, some results are derived by means of computational tools are illustrated numerically and depicted graphically.
Keywords: Heat conduction, internal heat sources, thin rectangular plate, deflection, stresses

1. INTRODUCTION

The theoretical problems of bending of the thin rectangular plate are used in a variety of engineering applications. Therefore, some theoretical studies concerning the problems of different edges, maybe clamped, simply supported, the temperature applied on different edges using different methods have been reported so far. The detailed thermal bending of thin plates has been stated in Nowinski's highly cited book (1978). Even studies on thermal stresses in two-dimensional (2D) or three-dimensional (3D) plates have also appeared many times. In this regard, Eslami et al. [1] in his book explained how to solve various boundary value problems of one-, two-, and three-dimension, and studied thermal stress of various structures, and improved the conclusion by numerical methods. Even, Misra [2] discussed a relatively simple paper in which upper surface was kept at a constant temperature while the lower surface, which is in contact with an elastic foundation with curved surface kept thermally insulated. Of most recent literature, some authors have undertaken the work on thermal stresses, which can be summarised as given below. Pachinger et al. [3] analyzed the thermally induced bending of thin rectangular plates with one clamped and three simply supported edges are studied for a spacewise constant thermal moment in this conclusion. Cheng et al. [4] on his paper discussed the analysis on Rectangular Thin Plate (RTP) having two opposite edges clamped, one edge simply supported and one edge free under temperature disparity is regarded as a superposition of the RTP of three simply supported edges and one edge free under temperature disparity and the RTP under the bending moment with two opposite edges. Zhong and Zhang [5] also investigated the RTP of three simply supported edges and one edge free under temperature disparity and the RTP under the bending moment with two opposite edges using condition related on small deflection theory and superposition principle, with consideration of temperature variation that is perpendicular to the surface. Deshmukh et al. [6] furnished a solution to the quasi-static problem of transient thermal bending stresses in a plate with the clamped edge using an integral transform. Few authors [7-11] have obtained different reports on the thermal bending analysis of the rectangular thin plate for various plate supports combinations. In previously referred papers, their objective was to maximize the load-carrying capacity of the structural support either by locating the supports or by changing stiffness. Hence, to the best of authors' knowledge, there exists scarce concentration on this topic of research in which internal heat source is taken into consideration the thermal bending moments. Things get further complicated when there exists a combination of internal heat generation and sectional heat supply is impacted on the body. Owing to the lack of research in this field, the authors have motived to conduct this study. In this paper, the realistic problem of a thin rectangular with an internal source in consideration subjected to prescribed surface temperature is studied. The theoretical calculation has been considered using the dimensional parameter, whereas graphical calculations are carried out using the dimensionless parameter. The success of this novel research mainly lies on the new mathematical procedures which present a much more straightforward approach for optimization of the design in terms of material usage and performance in engineering problem, particularly in the determination of thermoelastic behaviour in plate engaged as the foundation of pressure vessels, furnaces, etc.

2. FORMULATION OF THE PROBLEM

— Temperature distribution

Let us consider the rectangular plate occupying the space

$$-a/2 \le x \le a/2, -b/2 \le y \le b/2, -h/2 \le z \le h/2 \tag{1}$$

and its physical configuration in Cartesian coordinates can be shown in Figure 1 as

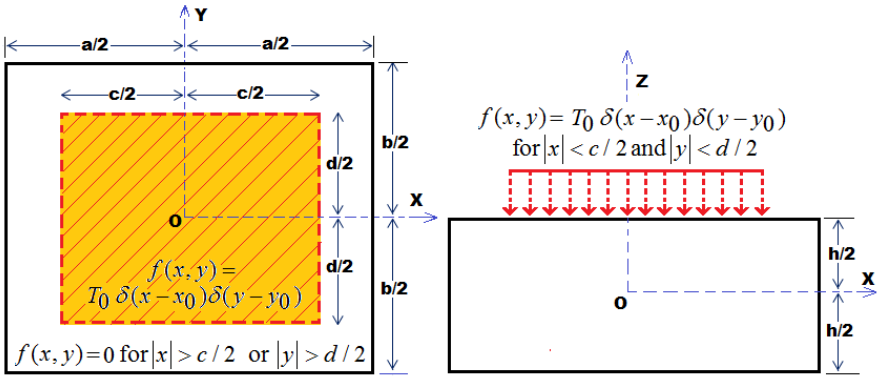

Figure 1. Schematic geometry of thick rectangular plate

We assume the expression for the unsteady temperature $T(x,y,z,t)$ as

$$T(x,y,z,t) = (z+h/2)\sum_{r=1}^{\infty}\sum_{s=0}^{\infty}\{[f_{rs}(t)\cos\alpha_r x\cos\beta_s y - z(z+h/2)] + x^2y^2\} \tag{2}$$

in which

$$\alpha_r = r\pi/a\,(r=1,3,5,\ldots), \tag{3}$$

$$\beta_s = 2s\pi/b\,(s=0,2,4\ldots), \tag{4}$$

and $f_{rs}(t)$ can be determined from the governing heat conduction equation.

The governing equation for unsteady-state heat conduction in isotropic solids is given as

$$\frac{\partial^2 T}{\partial x^2}+\frac{\partial^2 T}{\partial y^2}+\frac{\partial^2 T}{\partial z^2}+\mathrm{Q}=\frac{1}{\kappa}\frac{\partial T}{\partial t} \tag{5}$$

subjected to a partially distributed sectional heat supply on the top face

$$T\Big|_{\substack{z=h/2\\ t=0}} = f(x,y) \tag{6}$$

in which the prescribed surface temperature on top face is taken as

$$f(x,y)=\begin{cases} T_0\,\delta(x-x_0)\delta(y-y_0) & \text{for } |x|<c/2 \text{ and } |y|<d/2 \\ 0 & \text{for } |x|>c/2 \text{ or } |y|>d/2 \end{cases} \tag{7}$$

where T_0 being a constant temperature at $t=0$, thermal diffusivity is denoted as $\kappa=\lambda/\rho C$, λ being the thermal conductivity of the material, ρ is the density and C is the calorific capacity, which is assumed to be temperature-independent, respectively. The point impulsive sectional heat supply is represented as $\delta(x-x_0)\delta(y-y_0)$ for $-c/2<x_0<c/2$, $-d/2<x_0<d/2$ and the internal heat generation expressed in algebraic form as $Q=2[(h+3z)-x^2-y^2]$.

Since boundary condition of all the four edges (i.e. $x=\pm a/2$ and $y=\pm b$) are at zero temperature with arguments given in Eqs. (3)-(4) must automatically satisfy. Now it is enough for the analysis to satisfy boundary condition (7) and another boundary condition at bottom face (i.e. $z=-h/2$) having zero temperature.

Putting Eqs. (3) in (5) results in

$$\frac{\partial f(t)}{\partial t} = -\kappa(\alpha_r^2+\beta_s^2)f(t) \tag{8}$$

The above equation on integrating gives

$$f(t) = \mu_{rs}\,e^{-\kappa(\alpha_r^2+\beta_s^2)t} \tag{9}$$

in which μ_{rs} is the constant to be determined from the nature of temperature prescribed on the upper face. Using Eq. (7) and imposing boundary condition (6) on temperature change Eq. (2), we obtain

$$T_0\,\delta(x-x_0)\delta(y-y_0)=h\,[x^2y^2-(h^2/2)+1]\sum_{r=1}^{\infty}\sum_{s=0}^{\infty}\mu_{rs}\cos\alpha_r x\cos\beta_s y \tag{10}$$

On expanding $f(x,y)$ of Eq. (7) into a Fourier series, one obtains

$$\mu_{rs}=\frac{4T_0}{cdh[x_0^2y_0^2+1-(h^2/2)]} \tag{11}$$

Hence the required temperature distribution

$$T(x,y,z,t)=\begin{cases}(z+h/2)\sum_{r=1}^{\infty}\sum_{s=0}^{\infty}[\mu_{rs}e^{-\kappa(\alpha_r^2+\beta_s^2)t}\cos\alpha_r x\cos\beta_s y-z(z+h/2)]+x^2y^2 & \\ \qquad\qquad\qquad\qquad\qquad\qquad\qquad\qquad \text{for } |x|<c/2 \text{ and } |y|<d/2 & \\ 0 \qquad\qquad\qquad\qquad\qquad\qquad\qquad\qquad \text{for } |x|>c/2 \text{ or } |y|>d/2 & \end{cases} \tag{12}$$

The above result gives thermally induced resultant moment as

$$\begin{aligned}M_T&=\alpha E\int_{-h/2}^{h/2}z\,T(x,y,z,t)dz\\&=\alpha E\sum_{r=1}^{\infty}\sum_{s=0}^{\infty}[(h^4/24)\mu_{rs}e^{-\kappa(\alpha_r^2+\beta_s^2)t}\cos\alpha_r x\cos\beta_s y-(h^6/80)]\end{aligned} \tag{13}$$

and the resultant force as

$$\begin{aligned}N_T&=\alpha E\int_{-h/2}^{h/2}T(x,y,z,t)dz\\&=\alpha E\sum_{r=1}^{\infty}\sum_{s=0}^{\infty}[(h^3/12)\mu_{rs}e^{-\kappa(\alpha_r^2+\beta_s^2)t}\cos\alpha_r x\cos\beta_s y-(h^5/30)]+h\,x^2y^2\end{aligned} \tag{14}$$

in which α and E represents the coefficient of linear thermal expansion and Young's Modulus of the material of the plate, respectively.

The equation of equilibrium for the normal deflection in the absence of external load can be given as

$$D\nabla_1^4\omega+\rho h\frac{\partial^2\omega}{\partial t^2}=-\frac{\nabla_1^2M_T}{(1-\upsilon)} \tag{15}$$

and the associated boundary conditions of the plate are given as

$$\left.\begin{aligned}&\omega\big|_{t=0}=0,\ \left.\frac{\partial\omega}{\partial t}\right|_{t=0}=0,\ \text{for } -a/2\le x\le+a/2 \text{ and } -b/2\le y\le+b/2\\&\omega\big|_{x=\pm a/2}=0, \qquad \text{for all } y \text{ in } -b/2\le y\le+b/2\\&\omega\big|_{y=\pm b/2}=0, \qquad \text{for all } x \text{ in } -a/2\le x\le+a/2\\&\left.\frac{\partial^2\omega}{\partial x^2}+\frac{M_T}{(1-\upsilon)D}\right|_{x=\pm a/2}=0,\ \left.\frac{\partial^2\omega}{\partial y^2}+\frac{M_T}{(1-\upsilon)D}\right|_{y=\pm b/2}=0\end{aligned}\right\} \tag{16}$$

where $\omega(x,y,t)$ is the normal transverse deflection along z-direction of the midsurface, ∇_1^2 indicates the Laplacian operator, ∇_1^4 denotes the bi-harmonic operator, ρ the density of the material, constant υ denotes the Poisson's ratio of the disk, D is the flexural stiffness terms given as $D=E\ell^3/12(1-\upsilon^2)$ and the inertia loading term is taken as $\rho h(\partial^2\omega/\partial t^2)$.

Furthermore, the thermal stress components are written in the following form

$$\begin{aligned}\sigma_{xx}&=\frac{1}{h}N_x+\frac{12z}{h^3}M_x+\frac{1}{1-\upsilon}\left(\frac{1}{h}N_T+\frac{12z}{h^3}M_T-\alpha ET\right)\\\sigma_{yy}&=\frac{1}{h}N_y+\frac{12z}{h^3}M_y+\frac{1}{1-\upsilon}\left(\frac{1}{h}N_T+\frac{12z}{h^3}M_T-\alpha ET\right)\\\sigma_{zz}&=\frac{1}{h}N_{xy}-\frac{12z}{h^3}M_{xy}\end{aligned} \tag{17}$$

in which the resultant bending moments per unit length are given as

$$M_x = -D\left(\frac{\partial^2\omega}{\partial x^2}+\upsilon\frac{\partial^2\omega}{\partial y^2}\right)-\frac{M_T}{1-\upsilon},$$
$$M_y = -D\left(\frac{\partial^2\omega}{\partial y^2}+\upsilon\frac{\partial^2\omega}{\partial x^2}\right)-\frac{M_T}{1-\upsilon}, \quad (18)$$
$$M_{xy} = D(1-\upsilon)\frac{\partial^2\omega}{\partial x\partial y}$$

moreover, resultant forces per unit length are defined as

$$N_X = \frac{\partial^2 F}{\partial x^2},\ N_y = \frac{\partial^2 F}{\partial y^2},\ Nxy = -\frac{\partial^2 F}{\partial x\partial y} \quad (19)$$

which must satisfy

$$\frac{\partial N_X}{\partial x}+\frac{\partial N_{xy}}{\partial y}=0,\ \frac{\partial N_{xy}}{\partial x}+\frac{\partial N_y}{\partial y}=0 \quad (20)$$

where the stress function F can be obtained from

$$\nabla_1^4 F = -\nabla_1^2 N_T \quad (21)$$

The Eqs. (1)-(27) constitutes the mathematical formulation of the problem under consideration.

— **Solution of the Problem**

Firstly, we assume the expression for a transient thermal deflection given in Eq. (15) subjected to initial conditions expressed in the first equation of Eq. (16), as

$$w(x,y,t) = \sum_{r=1}^{\infty}\sum_{s=0}^{\infty}\phi_{rs}(t)\cos\alpha_r x\sin\beta_s y \quad (22)$$

Inserting the above result represented by Eq. (22) in Eq. (15), we deduce the differential equation satisfied by $\phi_{rs}(t)$ as

$$\frac{\partial^2\phi_{rs}(t)}{\partial t^2}+\lambda_{rs}^2\phi_{rs}(t) = \lambda_0 e^{-\kappa(\alpha_r^2+\beta_s^2)t} \quad (23)$$

in which $\lambda_{rs}^2 = \frac{D(\alpha_r^2+\beta_s^2)^2}{h\rho},\ \gamma_{rs} = \kappa(\alpha_r^2+\beta_s^2),\ \lambda_0 = \frac{\alpha E\gamma_{rs}h^2(2h^2-5\mu_{rs})}{60(1-\upsilon)\rho},$

with $\phi_{rs}''(t)=\phi_{rs}(t)=0$ at $t=0$.

Applying Laplace transforms to Eq. (23) and using the first equation of Eq. (16), one obtains

$$\bar{\phi}_{rs}(s) = \lambda_0\left\{\frac{1}{s(s+\gamma_{rs})(s+\lambda_{rs}^2)}\right\} \quad (24)$$

Now, applying inverse Laplace theorem to Eq. (24), one obtains

$$\phi_{rs}(t) = \lambda_0\left\{\frac{1}{\gamma_{rs}\lambda_{rs}^2}+\frac{e^{-\gamma_{rs}t}}{\gamma_{rs}(\gamma_{rs}-\lambda_{rs}^2)}+\frac{e^{-\lambda_{rs}^2 t}}{\lambda_{rs}^2(\gamma_{rs}-\lambda_{rs}^2)}\right\} \quad (25)$$

Hence the thermal deflection can be obtained by replacing Eq. (25) into Eq. (22) as

$$w = \frac{\alpha Eh^4\kappa}{60D(1-\upsilon)}\sum_{r=1}^{\infty}\sum_{s=0}^{\infty}\frac{\mu_{rs}}{(\alpha_r^2+\beta_s^2)^2}\left\{\frac{\rho he^{-\kappa(\alpha_r^2+\beta_s^2)t/\rho h}}{\alpha_r^2+\beta_s^2-\kappa\rho h}+\frac{1}{\kappa}\left[1-\frac{(\alpha_r^2+\beta_s^2)e^{-\kappa(\alpha_r^2+\beta_s^2)t}}{\alpha_r^2+\beta_s^2-\kappa\rho h}\right]\right\} \quad (26)$$
$$\times\cos\alpha_r x\sin\beta_s y$$

It is prominent from Eqs. (13) and (26) that the related boundaries are given in (16) on $x=\pm a/2, y=\pm b/2$ are evidently satisfied. Now inserting the above result given in Eq. (26) into Eq. (18), then in Eq. (17) taking all resultant forces given in Eq. (19) as zero, we get the desired thermal bending stresses as

$$\sigma_{xx}=\frac{1}{60(-1+\upsilon)}\sum_{r=1}^{\infty}\sum_{s=0}^{\infty}\frac{2h^4-30E\alpha z(z+h/2)+60x^2y^2(-1+E\alpha)}{(\alpha_r^2+\beta_s^2)^2(\alpha_r^2+\beta_s^2-\kappa\rho h)}$$
$$+\frac{1}{(\alpha_r^2+\beta_s^2)^2(\alpha_r^2+\beta_s^2-\kappa\rho h)}\Big\{E\alpha\mu_{rs}e^{-(\alpha_r^2+\beta_s^2)(\alpha_r^2+\beta_s^2+2\kappa\rho h)t/\rho h}\cos\alpha_r x$$
$$\times\Big[-5e^{\kappa(\alpha_r^2+\beta_s^2)(\alpha_r^2+\beta_s^2+\kappa\rho h)t/\rho h}[(-6+h)h-12z](\alpha_r^2+\beta_s^2)(\alpha_r^2+\beta_s^2-\kappa\rho h)$$
$$\times\cos\beta_s y+12hz\alpha^2(1+\upsilon)\Big(e^{(\alpha_r^2+\beta_s^2)(\alpha_r^2+\beta_s^2+\kappa\rho h)t/\rho h}(\alpha_r^2+\beta_s^2)$$
$$-e^{2\kappa(\alpha_r^2+\beta_s^2)t}h\kappa\rho-e^{(\alpha_r^2+\beta_s^2)(\alpha_r^2+\beta_s^2+2\kappa\rho h)t/\rho h}(\alpha_r^2+\beta_s^2+\kappa\rho h)\Big)$$
$$\times\sin\alpha_r y\Big]\Big\} \tag{27}$$

$$\sigma_{yy}=\frac{1}{60(-1+\upsilon)}\sum_{r=1}^{\infty}\sum_{s=0}^{\infty}\frac{2h^4-30E\alpha z(z+h/2)+60x^2y^2(-1+E\alpha)}{(\alpha_r^2+\beta_s^2)^2(\alpha_r^2+\beta_s^2-\kappa\rho h)}$$
$$+\frac{1}{(\alpha_r^2+\beta_s^2)^2(\alpha_r^2+\beta_s^2-\kappa\rho h)}\Big\{E\alpha\mu_{rs}e^{-\kappa(\alpha_r^2+\beta_s^2)(\alpha_r^2+\beta_s^2-\kappa\rho h)t/\rho h}\cos\alpha_r x$$
$$\times\Big[-5e^{\kappa(\alpha_r^2+\beta_s^2)(\alpha_r^2+\beta_s^2+\kappa\rho h)t/\rho h}[(-6+h)h-12z](\alpha_r^2+\beta_s^2)(\alpha_r^2+\beta_s^2-\kappa\rho h)$$
$$\times\cos\beta_s y+12hz\alpha^2(1+\upsilon)\Big(e^{(\alpha_r^2+\beta_s^2)(\alpha_r^2+\beta_s^2+\kappa\rho h)t/\rho h}(\alpha_r^2+\beta_s^2)$$
$$-e^{2\kappa(\alpha_r^2+\beta_s^2)t}h\kappa\rho-e^{(\alpha_r^2+\beta_s^2)(\alpha_r^2+\beta_s^2+\kappa\rho h)t/\rho h}(\alpha_r^2+\beta_s^2+\kappa\rho h)\Big)$$
$$\times\sin\alpha_r y\Big]\Big\} \tag{28}$$

$$\sigma_{zz}=\frac{\alpha Eh\kappa}{5}\sum_{r=1}^{\infty}\sum_{s=0}^{\infty}\frac{z\alpha_r^2\mu_{rs}}{(\alpha_r^2+\beta_s^2)^2}\Big\{\frac{\rho he^{-\kappa(\alpha_r^2+\beta_s^2)t/\rho h}}{\alpha_r^2+\beta_s^2-\kappa\rho h}+\frac{1}{\kappa}\Big[1-\frac{(\alpha_r^2+\beta_s^2)e^{-\kappa(\alpha_r^2+\beta_s^2)t}}{\alpha_r^2+\beta_s^2-\kappa\rho h}\Big]\Big\} \tag{29}$$
$$\times\sin\alpha_r x\cos\beta_s y$$

3. NUMERICAL RESULTS, DISCUSSION AND REMARKS

For the sake of simplicity of calculation, we set the functions as

$$\bar{x}=[x-(-a/2)]/a,\bar{y}=[y-(-b/2)]/a,\bar{z}=[z-(-\ell/2)]/a,$$
$$\tau=\kappa t/a^2,T(x,y,z,t)=T(x,y,z,t)/T_0,\bar{W}=W/\alpha T_0 a \tag{30}$$
$$\bar{\sigma}_{ij}=\sigma_{ij}/E\alpha_t\theta_k\quad(i,j=x,y)$$

Substituting the dimensionless value of Eq. (30) in temperature distribution Eq. (12), thermal deflection Eq. (26) and in components of stresses Eqs. (27)-(29), we obtained the desired expressions for our numerical discussion.

The numerical computations have been carried out for Aluminum elliptical plate with physical parameter as length $a=2.5$ m, breadth $b=2$ m, height $\ell=0.08$ m, and reference temperature as 150 ^{0}C. The thermo-mechanical properties are considered as modulus of elasticity $E=70$ GPa, Poisson's ratio $\upsilon=0.35$, thermal expansion coefficient $\alpha=23\times10^{-6}$ /^{0}C, thermal diffusivity $\kappa=84.18\times10^{-6}$ m^{2}s^{-1} and thermal conductivity $\lambda=204.2$ Wm^{-1}K^{-1}.

In order to examine the influence of heating on the plate, the numerical calculations were performed for all the variables, and numerical calculations are depicted in the following figures with the help of MATHEMATICA software.

Figs. 2–4 illustrates the numerical results of temperature, stresses and the deflection of the plate due to interior heat generation within the solid, under thermal boundary condition that are subjected to a known initial surrounding temperature at any particular instance.

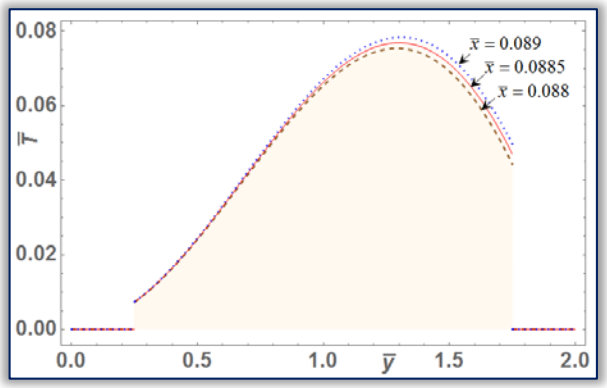

Figure 2 (a): Temperature distribution along $\bar{x}$ - direction for different values of $\bar{z}$.

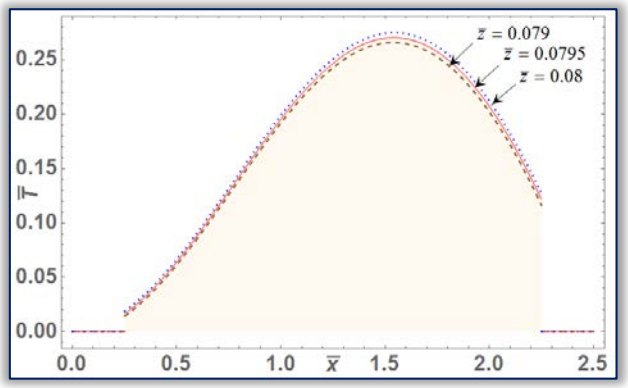

Figure 2 (b): Temperature distribution along $\bar{y}$ - direction for different values of $\bar{x}$.

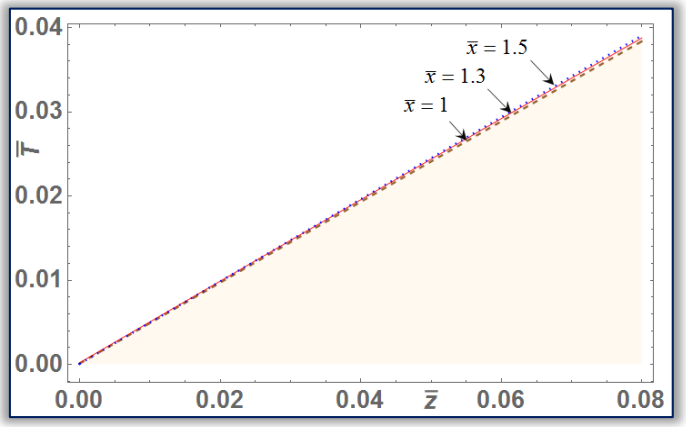

Figure 2 (c): Temperature distribution along $\bar{z}$ -direction for different values of $\bar{x}$.

In Figures 2(a)-2(c), the dimensionless temperature distribution increases along $(\bar{x}, \bar{y}, \bar{z})$ – direction of the plate with internal heat supply are depicted. At the central part of the length and breadth, temperature fluctuation attains maximum and it may be due to available accumulation of energy of internal heat source and hence thermal expansion is more at the central part of the plate, giving high tensile force, as shown in Figure 2(a). Figure 2(b) also shows the variation in the temperature profile along $(\bar{x}, \bar{y}, \bar{z})$ – direction for various location of thickness and it is observed that nature is similar to that of trend shown in Figure 2(a) except the magnitude. Figure 2(c) illustrates the temperature profile along the axial direction for different points along $\bar{x}$ – direction and it is observed that the temperature trend increases linearly along the $\bar{z}$ – direction towards the outer edge due to the thinness structure. From the physical point of view, the internal heat source in combination of sectional heat supply plays a role of heat source for the temperature distribution if the

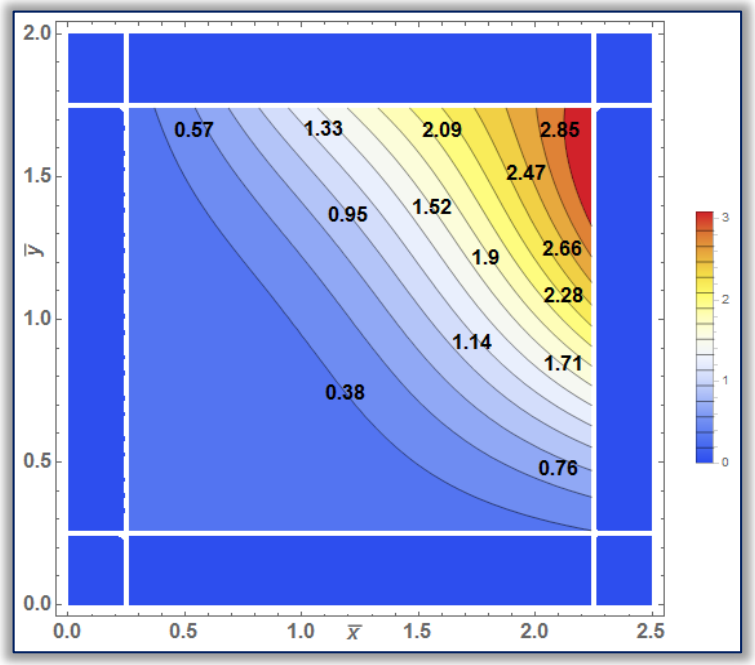

Figure 2 (d): Contour plot of temperature distribution along $\bar{x}\,\bar{y}$ – plane for a fixed value of $\bar{z}$.

generation rate $(Q>0)$ is positive and it acts as a heat sink if the generation rate $(Q<0)$ is negative. The result agrees with the previous result [12]. Figure 2(d) shows the temperature distribution in isolines contour plot along $\bar{x}\,\bar{y}-$ plane which shows a combined effect of Figure (2a)-(2b) for fixed location along the axial direction.

Figure 3(a) depicts thermal deflection along the $\bar{y}-$direction at different location of $\bar{x}$, and it was observed that the thermal deflection gradually increases within the rectangular frame due to the available internal heat source and sectional supply. Figure 3(b) illustrates that the absolute value of thermal deflection increases with time for the simply-supported edge. Initially, the deflection increases gradually, and it attains maximum expansion due to the accumulation of thermal energy dissipated by internal heat generation and point impulsive heat supply.

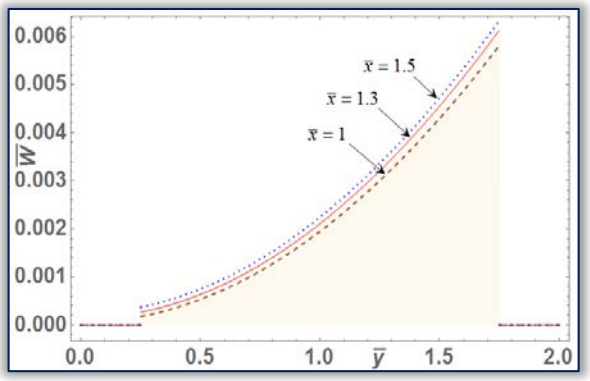

Figure3 (a): Deflection along $\bar{y}-$direction for different values of $\bar{x}$.

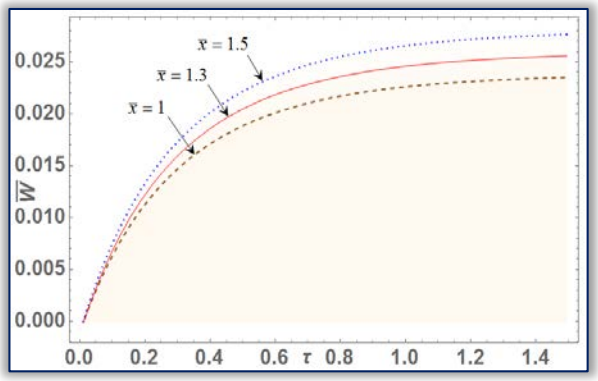

Figure 3 (b): Deflection along time-direction for different values of $\bar{x}$.

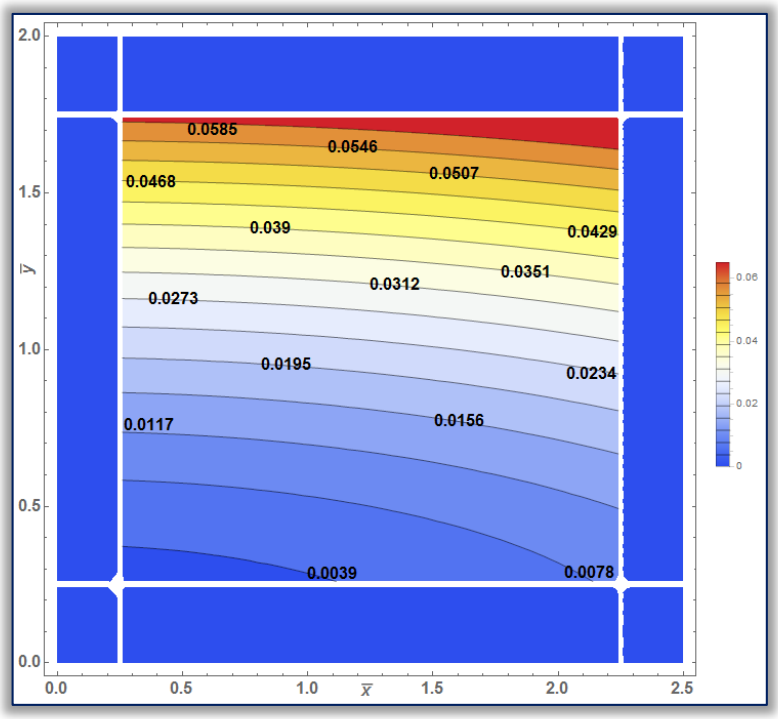

Figure 3 (d): Contour plot of deflection along $\bar{x}\,\bar{y}-$ plane for a fixed value of τ.

From Figure 3(c), one can see the thermal deflection in isolines contour plot along $\bar{x}$ and $\bar{y}-$ directions at a fixed dimensionless time τ, in which the darkly shaded portion agrees with the graph plotted in Figure 3(a). The defection in the red area near the outer edge shows maximum displacement, maybe due to the internal heat source and sectional heat supply, while blue colour area indicates the zero deflection at the outer region of the rectangular frame.

Figs. 4(a)-4(d) shows the characteristic nature of dimensionless thermal stresses in a rectangular plate which is impacted by point impulsive heat source and having internal heat generation. The distribution profile is shown in Figure 4(a) is at zero value which gradually decreases towards the outer part and attains maximum due to accumulation heat energy obtained from the external sectional heat supply and internal heat generation, then it again attains zero at the unheated region. Figure 4(a) shows a similar trend in Figure 4(b) in which $\bar{\sigma}_{xx}$ profile shows minimum value due to the compressive force is occurring at the starting end of heated region and gradually tensile forces increase the magnitude towards the outer part.

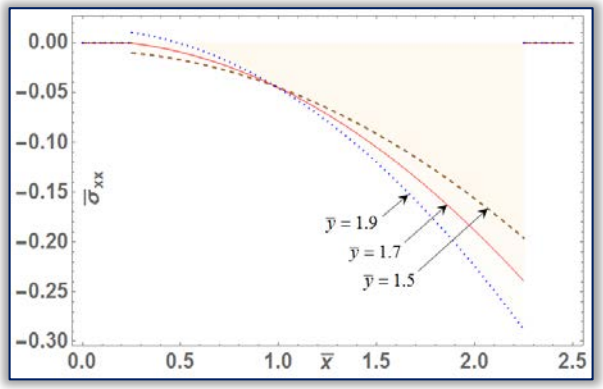

Figure 4 (a): Thermal stresses $\bar{\sigma}_{xx}$ along $\bar{x}-$ direction for different values of $\bar{y}$.

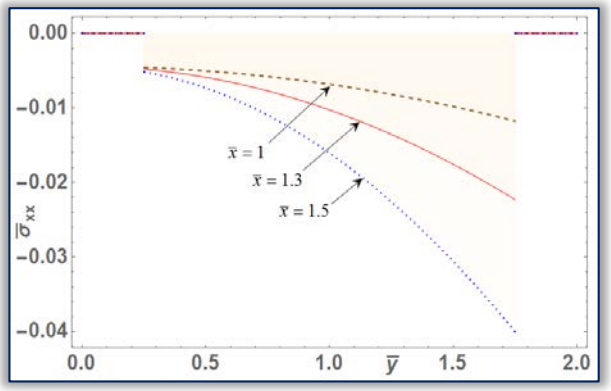

Figure 4 (b): Thermal stresses $\bar{\sigma}_{xx}$ along $\bar{y}-$ direction for different values of $\bar{x}$.

Figure 4(a) shows $\bar{\sigma}_{xx}$ profile illustrates that more compressive stress occurring at the inner part which goes on increasing towards positive magnitude along $\bar{x}-$ direction and it attains a maximum at the outer edge. $\bar{\sigma}_{yy}$ and $\bar{\sigma}_{zz}$ has a maximum tensile stress at the outer surface, whereas the compressive stress is occurring on the all the four edges (i.e. for $\bar{x}$ and $\bar{y}$) are at zero temperature. A similar trend is also observed in Figure 4(b) and the increment in the stress may be due to the increase in the rate of heat propagation which initially leads to compressive force and expands more as distance decrease towards the section heat supply.

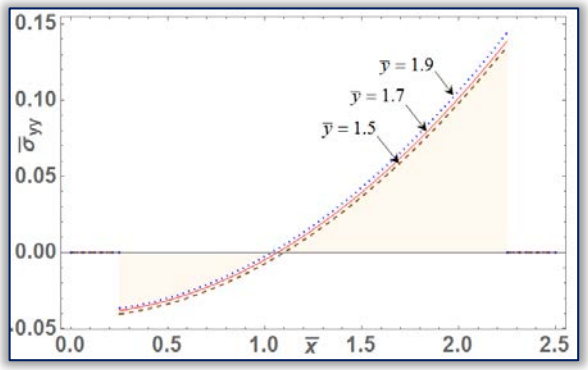

Figure 4 (b): Thermal stresses $\bar{\sigma}_{yy}$ along $\bar{x}-$ direction for different values of $\bar{y}$.

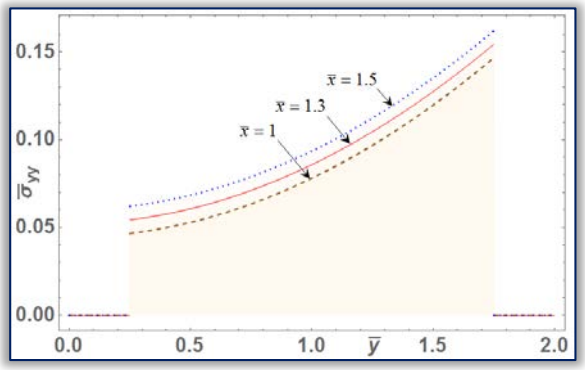

Figure 4 (c): Thermal stresses $\bar{\sigma}_{yy}$ along $\bar{y}-$ direction for different values of $\bar{x}$.

The dimensionless thermal stress $\bar{\sigma}_{zz}$ has maximum tensile stress at the outer surface, whereas the compressive stress is occurring on all the inner edges (i.e. for $\bar{x}$ and $\bar{y}$), and zero stresses at the unheated region.

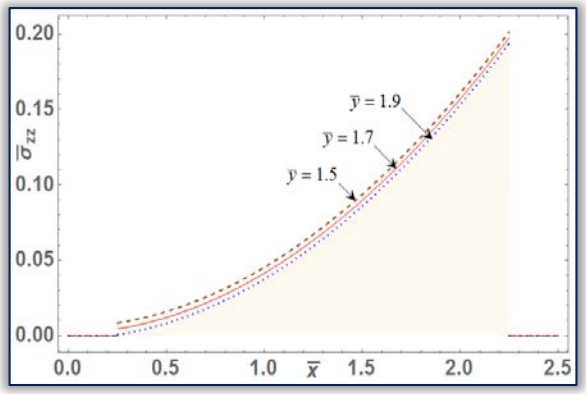

Figure 4 (d): Thermal stresses $\bar{\sigma}_{zz}$ along $\bar{x}-$ direction for different values of $\bar{y}$.

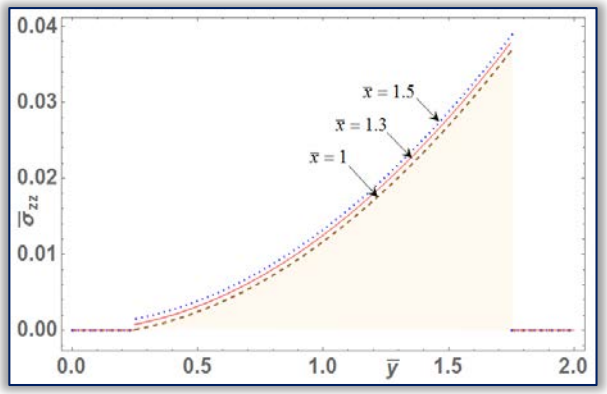

Figure 4 (d): Thermal stresses $\bar{\sigma}_{zz}$ along $\bar{y}-$ direction for different values of $\bar{x}$.

4. CONCLUSIONS

The unsteady-state thermal bending of a thin rectangular plate subjected to a partially distributed temperature on the top face was analyzed by a classical method. The boundary condition of all the four edges (i.e. $x = \pm a/2$ and $y = \pm b$) and another boundary condition at bottom face (i.e. $z = -h/2$) are kept at zero temperature with proper arguments that rigorously were satisfied. The method followed to obtain the solution can be applied with ease to other thermal bending problem like moderately thick rectangular plates with simply-supported or clamped edges or so. From the results of the numerical calculations for the thin rectangular plate, the following conclusions may be drawn.

- The advantage of this classical approach is its generality and its mathematical power to handle different types of mechanical and thermal boundary conditions during small deflection under partial thermal loading.
- The maximum tensile stress shifting towards mid-core from inner and outer surfaces of the plate. This could be due to heat and stresses available due to internal heat sources under known sectional heat supply.
- Initially, the value of stresses of all the four edges and bottom are zero as per the proposed prescribed surface temperature, and it attains maximum bending stress at mid-core. The effect of stretching on the stresses is stronger than that of bending [1].
- Neglecting the inertia term from Eq. (15), we get the static solution of small deflection.
- The aforesaid bending analysis concept can be beneficial in the field of micro-devices or microsystem applications, planar continuum robots, predicting the elastoplastic bending and so forth.

References

[1] M.R. Eslami, R.B., Hetnarski, J. Ignaczak, N. Noda, N. Sumi, and Y. Tanigawa, Theory of elasticity and thermal stresses, Springer Netherlands, Vol. 197, pp. 513–533, 2013.
[2] J.C. Misra, On the thermal bending of a thin elastic simply supported rectangular plate resting on an elastic foundation, Pure and Applied Geophysics, Vol. 112, No. 1, pp. 83-89, 1974.
[3] F. Pachinger and H. Lrschik, Fast convergent series solutions for thermal bending of thin rectangular plates, Journal of Thermal Stresses, Vol. 21, No. 7, pp. 763–775, 1998.
[4] X.S. Cheng and Y.F. Du, The discussion of the analytical solution about rectangular thin slab under temperature disparity with four simply supported edges, Low Temperature Architecture Technology, Vol. 28, No. 4, pp. 76–78, 2006.
[5] Y. Zhong and Y.S. Zhang, Theoretic solution for rectangular thin plate with arbitrary boundary conditions by symplectic geometry method, Chinese Journal of Applied Mechanics, Vol. 22, No. 2, pp. 293–297, 2005.
[6] K.C. Deshmukh, M.V. Khandait, S.D. Warbhe and V.S. Kulkarni, Thermal stresses in a simply supported plate with thermal bending moments, International Journal of Applied Mathematics and Mechanics, Vol. 6, No. 18, pp. 1–12, 2010.
[7] Y. Zhong, R. Li, Y. Liu and B. Tian, On new symplectic approach for exact bending solutions of moderately thick rectangular plates with two opposite edges simply supported, International Journal of Solids and Structures, Vol.46, No. 11-12, pp. 2506–2513, 2009.
[8] X. Cheng and J. Fan, Thermal bending of rectangular thin plate with two opposite edges clamped, one edge simply supported and one edge free, KSCE Journal of Civil Engineering, Vol. 20, No. 1, pp. 333–342, 2016.
[9] X. Cheng, J. Nie, L. Zhao and W. Shi, The thermal bend of RTP with one edge clamped and two edges simply supported and one edge free, Archive of Applied Mechanics, Vol. 85, No. 2, pp. 287–302, 2015.
[10] X. Cheng and J. Fan, Thermal bending of rectangular thin plate with two opposite edges clamped, one edge simply supported and one edge free, KSCE Journal of Civil Engineering, Vol. 20, No. 1, pp. 333–342, 2015.
[11] X. Cheng, J. Nie, L. Zhao and W. Shi, The thermal bend of RTP with one edge clamped and two edges simply supported and one edge free, Archive of Applied Mechanics, Vol. 85, No.2, pp. 287–302, 2014.
[12] K.C. Deshmukh, M.V. Khandait, R. Kumar, Thermal stresses in a simply supported plate with thermal bending moments with heat sources, Materials Physics and Mechanics, Vol. 21, pp. 135-146, 2014.

ISSN 1584 – 2665 (printed version); ISSN 2601 – 2332 (online); ISSN-L 1584 – 2665